4. EXPERIMENTAL FACILITIES IN BEAM HALL

4.1 GENERAL PURPOSE SCATTERING CHAMBER (GPSC)

Golda K.S., A. Kothari, P. Barua, P. Sugathan, S.K. Datta and R.K. Bhowmik

A number of experiments both in Nuclear Physics as well as in Materials Science are conducted using this facility. As per the experimental requirements of the user community new developments are carried out. Recently we have installed a camera inside the chamber to get a better view of the components put inside the chamber like target ladder, detectors, etc. The performance of the camera under vacuum condition is tested satisfactorily.

Other than the developmental works, a number of activities are undertaken to assist in the experiments. Major support activities during the experiments include installation of different extra components such as re-entrant Gamma detector port, gas handling system, special flanges, extended beam dump, etc. to the chamber. The list of experiments carried out last year using this facility is given below.

Materials Science Experiments

User	Title	Beam	Energy (MeV)
D. Saikia Tezpur Univ.	Investigation of SHI irradiation effects on ionic conductions in Li based gel polymers electrolytes	C	50-70
Arun Batra ISRO	Heavy ion induced effects in VLSI Devices	B /Si Cl/Ag	100/100 120/65
A.P. Hussain Tezpur University	Effect of SHI irradiation on intrinsic conducting polymers	Cl	100
J.K. Quamara NIT, Kurukshetra	Optoelectronic processes in ion irradiated polymers	Au	150
Saif. A. Khan NSC	Transition from cooling to heating of ions transmitted through a crystal.	Ni Pulsed	90
Rajesh Kumar AMU, Aligarh	Characterization of SHI induced modification in polymers	Si	70-100
J.K. Quamara NIT, Kurukshetra	Relaxation processes in corona poled swift heavy ion irradiated polymers	I P	50
Y.K.Vijay University of Rajasthan	Development of nano-filters for gas permeation	Cl	150

Nuclear Physics Experiments

User	Title	Beam	Energy (MeV)
M.A. Ansari AMU, Aligarh	Study of incomplete fusion reactions induced by heavy ions	^{12}C ^{16}O	30-100
Tilak Ghosh SINP, Kolkata	Study of heavy ion induced fission fragment angular and mass distribution at near & sub-Coulomb barrier energies	^{16}O, ^{12}C pulsed	96-108 70-90
Jagdeep Kaur Panjab University	Study of dynamical & entrance channel effects in fusion reactions at high excitation energy & angular momentum	^{37}Cl ^{16}O ^{12}C	125 85 80
Tauseef Ahmad AMU, Aligarh	Study of heavy ion induced reactions at intermediate energies	^{16}O	60-100
S.K. Datta NSC	Study of neutron multiplicities in fission reactions	^{16}O Pulsed	96, 100, 105

4.1.1 Double Slit Controller

M. Archunan and P. Barua

A Remote controller is made for the double slit installed at the chamber entrance which controls the beam size for materials science experiments. This controller contains four identical stepper motor controllers to control the bidirectional motion of each slit; +X, -X, +Y, and -Y. Fig. 1 shows the front panel and internal circuitry of the slit controller. The movement is displayed as a four digit number. The displayed readings can be calibrated to the required units. The display shows only one channel at a time. But the channels can be selected at any time. To select the channel of the slit for display on the DPM, a display selector switch is provided. There is provision to control the direction of motion of each

Fig. 1 : Internal circuitry of the Double slit controller.

channel. A selector switch is provided to move the channels in or out. There are four separate run switches for each channel of the slit. To select the moving direction of the channel, there are four separate in/out switches for each channel of the slit. The LED indicators show in/out limits. This controller, placed in the Data Room enables an easy control of the double slit remotely.

4.1.2 GPSC in Beam Hall II

Golda K.S., A. Kothari, P. Barua, R.P. Singh, P. Sugathan, S.K. Datta and R.K. Bhowmik

We are planning to shift the General Purpose Scattering Chamber (GPSC) to the -40° beam line of the Phase II beam hall when accelerated beams from LINAC become available. The schematic layout of the beam line dedicated to Nuclear Physics experiments is shown in fig. 2. Apart from the GPSC, an array of neutron detectors (National Array of Neutron Detectors, NAND) would be set up by pooling the neutron detectors available at different institutions in the country. A thin walled spherical vacuum chamber of 60cm diameter and 3mm thickness of SS has been designed. The neutron detectors could be placed at a distance of 2m from the target position around this chamber while the charged particle detectors and gas detectors could be placed on sector plates inside the chamber. Beam will be dumped at a distance of 4m downstream from the target position.

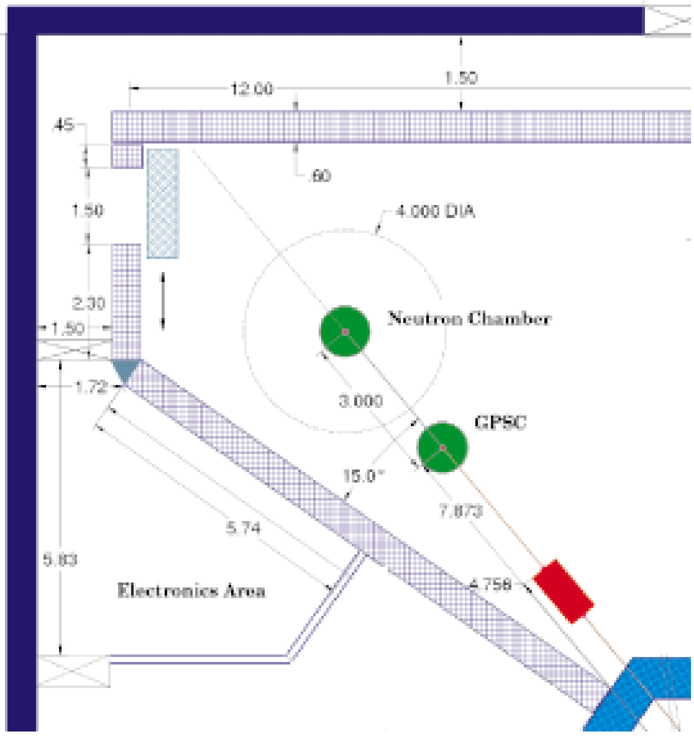

Fig. 2 : Schematic layout of GPSC beam line in Beam Hall II

4.1.3 Scattering Chamber for NAND

Golda K.S., J. Zacharias, A. Kothari, P. Barua, R.P. Singh, S.K. Datta and R.K. Bhowmik

For the measurement of neutron angular distribution, a thin-walled spherical chamber of 600mm diameter made of 3mm thick SS has been designed. The total allowable stress on a spherical shell of 3mm steel has been calculated and it has been found that the chamber dimension can hold the required vacuum conditions well within the safety limit. The chamber is designed along with associated accessories and the fabrication is going on. An isometric view of the designed chamber is given in fig. 3. The internal structure of the chamber, (fig. 4), is done in such a way that the detectors can be put at any desired distance at any angle with provision for both distance and angular read out.

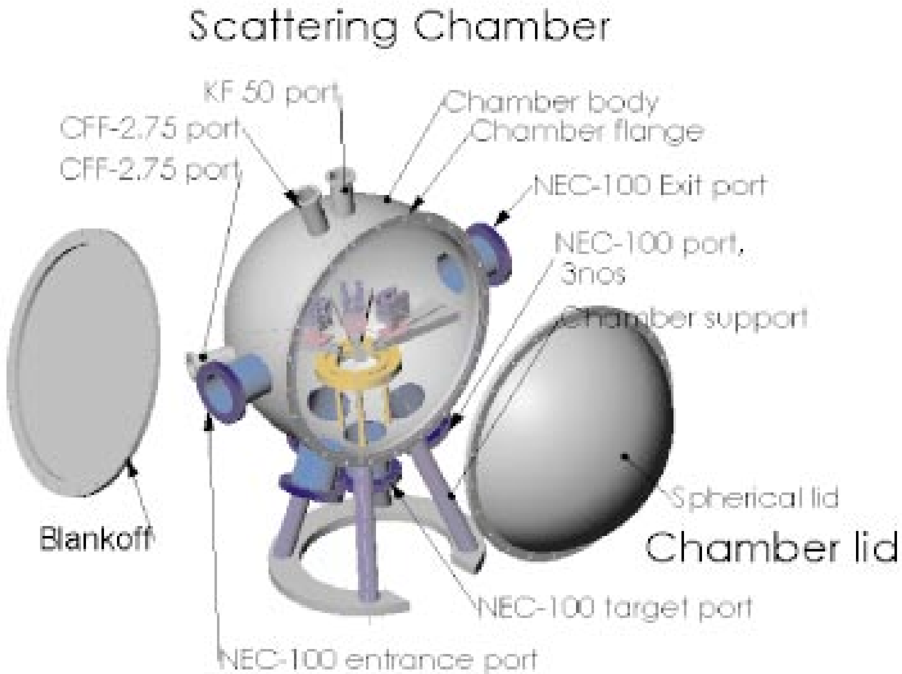

Fig. 3 : Isometric view of the scattering chamber

Salient Features of the Chamber:

1. Two asymmetric hemispherical parts for normal use.
2. A flat lid is provided for using gamma detectors along with neutron array.
3. Sector plates are made to put charged particle detectors, such as large area MWPC, Solid state detectors, Ionization chamber, etc inside the chamber.
4. Sector plates can be fixed at any desired angle; angular reading is possible.

5. Detectors can be kept at any distance from the target up to the chamber wall; distance marking is provided in the sector plates.
6. There is provision to put two monitor detectors at ±12° close to the beam exit port.
7. The target ladder comes from the 4" bottom port. There will be provision for linear and rotary movement of the target ladder.
8. All the electrical connections are taken through two 4" ports provided at 25° to the centre on the bottom part of the chamber.
9. A KF50 port is provided on the top for in-vacuum target transfer.
10. A 2" camera port is provided at 20° to the beam axis in the beam entrance side
11. A 2” view port is provided at 15° to the target ladder port on the top.
12. A 4" port at the bottom is provided for gas feed-throughs for gas detectors.

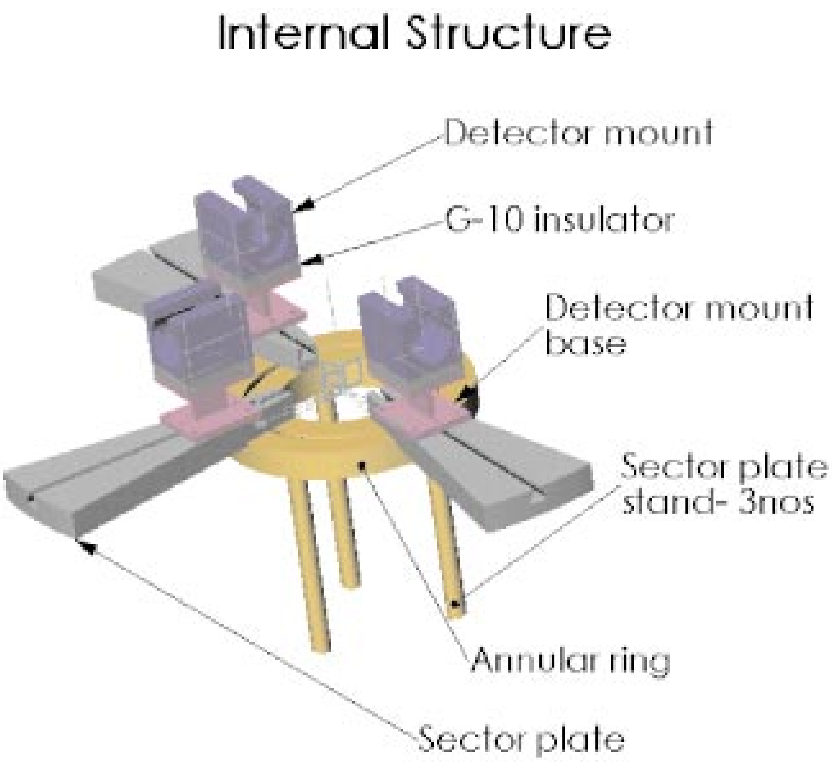

Fig. 4 : Internal structure of the chamber

Two Turbo pumps of 250 l/sec pumping capacity backed by oil free scroll pumps will be used to pump the chamber up to a vacuum of $1x10^{-6}$ torr. To minimize the number of ports in the chamber, pumping will be done through T’s connected to beam entrance and exit ports rather than having a pumping port in the chamber itself. The weight of the chamber is about 25 kg and it will be supported by a MS stand which will have provision for alignment in X, Y and Z directions. The beam dump connected to the exit port of the chamber will be 4m long in order to reduce the background neutrons from the beam dump seen by the neutron detectors.

4.1.4. Measurement of Neutron detector efficiency

Golda K.S., R.P. Singh, S.K. Datta and R.K. Bhowmik

Response function of neutron detectors of different types have been reported by several groups and it has been observed that it depends on the dimension, energy resolution and history of the detectors. Therefore it is always desirable to experimentally measure the efficiency of the detector rather than merely depending on theoretical calculations. An experiment is done to measure the relative detection efficiency of 5" dia X 5" thick BC501 liquid scintillation neutron detector by measuring energy spectra of prompt neutrons from a ^{252}Cf spontaneous fission neutron source using time of flight technique. The obtained TOF spectra are converted into energy spectra with proper application of Jacobian conversion. The limited velocity resolution of the detector due to its finite length is taken into account while determining the energy bin size of the spectrum. The obtained energy spectrum at a particular threshold setting is compared with the standard reported spectrum of ^{252}Cf to determine the relative neutron detection efficiency of the detector. The experimentally obtained relative efficiency, fig. 5, is compared with Monte Carlo calculations using the code MODEFF. A more detailed study has to be carried out to determine the absolute efficiency of these detectors with mono energetic neutrons.

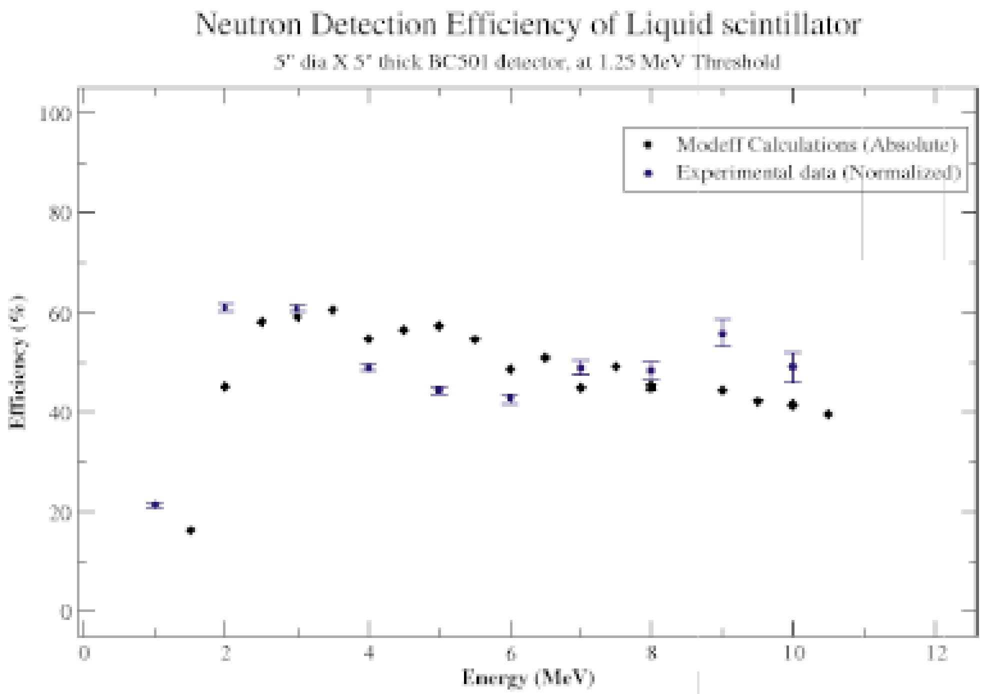

Fig. 5 : Neutron detection efficiency (relative) of liquid scintillator.

4.1.5 Large Area Position sensitive MWPC

Golda K.S., Ashok Kotari, P. Barua, P. Sugathan, Thomas Varughese and S.K. Datta.

The large area position sensitive MWPC fabricated for fission fragment detection is tested with both alpha and fission sources. The operating gas pressures and the biased voltages of the detector are optimized for both light particles as well as heavy fission fragments. To test the position resolution of the detector a mask made in G-10 sheet is put in front of the detector and the data is collected. The TOF spectrum generated between anode signal and the X-position signal shows clear peaks corresponding to 1mm holes in the mask, fig. 6. The detector is satisfactorily used in recent experiments for fission fragment mass measurements using Time of Flight techniques. The detector performance is good enough to separate fission events form other events e.g. elastic events. Y plane is also incorporated in the detector.

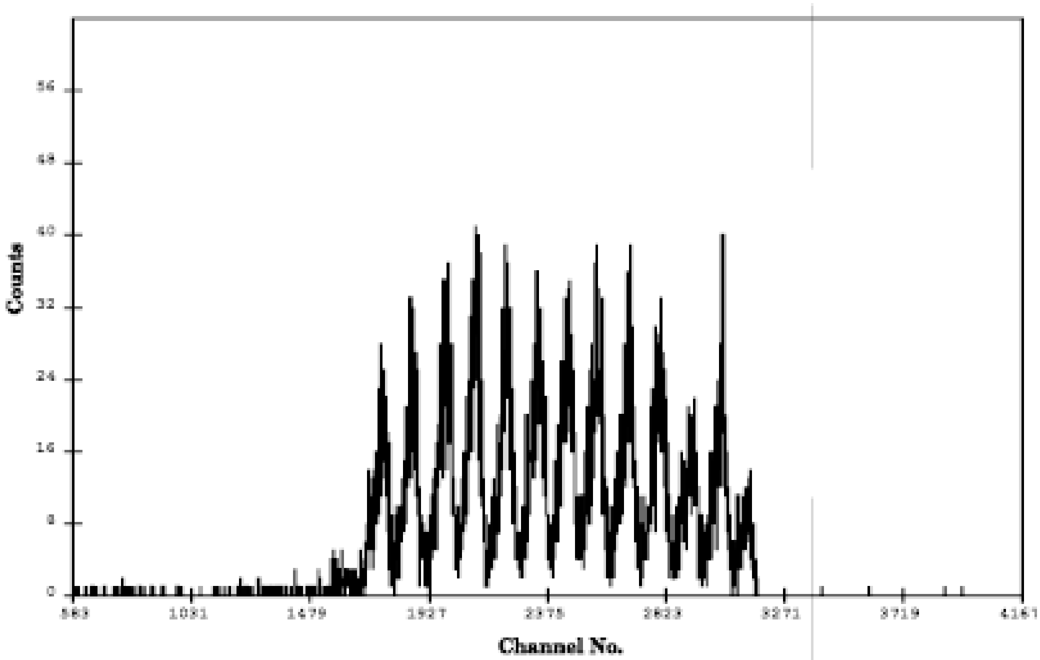

Fig. 6 : Position Spectrum obtained with mask.

4.1.6 Study of neutron multiplicity from fission reaction

Golda K.S.[1], Hardev Singh[2], P.D. Shidling[3], Pankaj Kumar[1], A Jhingan[1], R.P. Singh[1], P. Sugathan[1], I.M. Govil[2] and S.K. Datta[1]

[1]Nuclear Science Centre, New Delhi-110067.
[2]Panjab University, Chandigargh.
[3]Karnataka university, Dharwad.

Study of neutron emission in heavy ion induced fusion-fission reactions provides an excellent tool to study reaction time, temperature, etc. Pre and post-scission neutron multiplicities are used to compare fission time scales with neutron evaporation times. We have developed a facility for the measurement of neutrons emitted in fusion-fission reactions at Nuclear Science Centre. The in-beam test of the facility is carried out with pulsed ^{16}O on ^{197}Au target at different beam energies; at 96,100 and 105 MeV. Two large area position sensitive MWPCs are placed at folding angles to catch complimentary fission fragments simultaneously. These MWPCs give timing, energy loss, X- and Y-position signals. Two monitor detectors, 300 µm thick silicon surface barrier, kept at ±11° are used for beam flux normalization purpose. Two 5" diameter X 5" thick BC501 liquid scintillators kept at a distance of 1m from the target position, one along and the other perpendicular to the direction of fission fragments, are used for neutron detection. Beam is dumped about 8 feet downstream from the target in a paraffin shielded tantalum Faraday cup. A schematic diagram of the experimental set-up is shown in fig. 7.

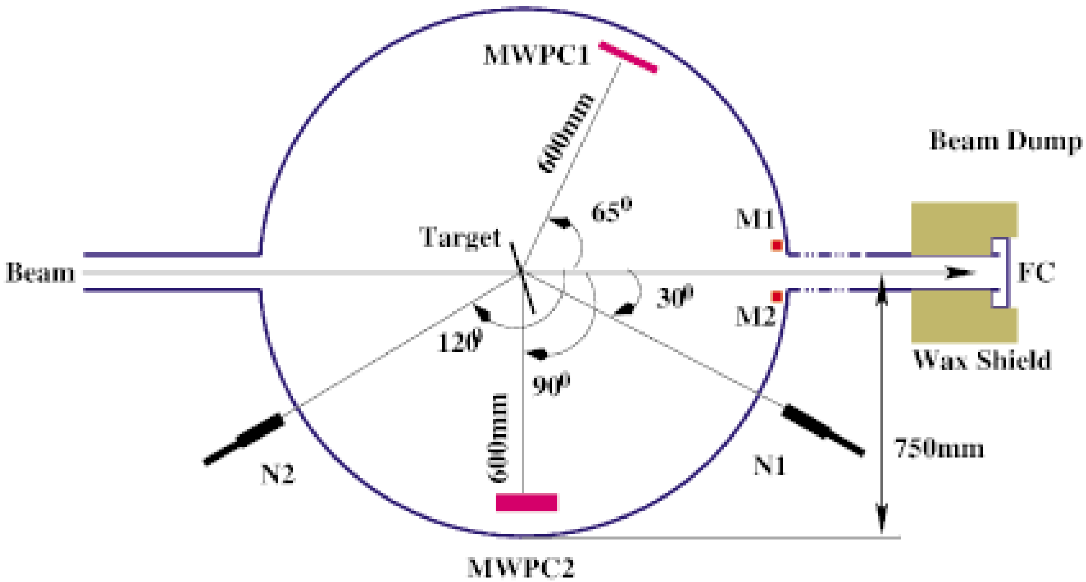

Fig. 7 : Schematics of the experimental set-up

Time of Flight (TOF) method is used to measure the energy of neutrons as well as the velocity of fission fragments. RF signal from the beam buncher is used as the time reference. For coincidence between any neutron detectors with any fission fragment detectors, the arrival times for neutrons and fission fragments were recorded with respect to the timing signal from the beam buncher. Neutron TOF spectra is collected by setting a cutoff of neutron energy of 0.5MeV by measuring the maximum Compton electron recoil energy using different gamma ray sources. Pulse shape discrimination technique is adapted for rejecting gamma rays detected by neutron detectors. Neutron energy spectra (fig. 8), are obtained from the measured TOF spectra after correcting for the neutron detector efficiency, obtained from Monte-Carlo calculations (MODEFF). The TOF flight measurements of the fission fragments are used to determine the mass distribution. Mass is obtained from the precise determination of the flight path, lab angles and TOF difference between the two complementary fragments, by assuming full momentum transfer to the compound nucleus and neglecting light particle emission from the fragments.

The performance of the fission detectors is tested satisfactorily and the operating parameters such as gas pressure of iso-butane used, applied bias, etc. are optimized. Successful setting up of the detector configuration, electronics and data collection technique for the neutron spectrum measurement in coincidence with fission fragments is achieved in this test experiment. The properties of energy distribution of fission neutrons in two different lab angles are studied. Pre- and post-scission neutron multiplicities are extracted from the neutron energy spectra by fitting it with Watt expression. These values match very well with the results in the literature. Fission folding angle for ^{16}O + ^{197}Au at 105 MeV lab energy is calculated and it matches well with the results in the literature. Mass distribution of the fission fragment is obtained with the peak at 112 amu and FWHM of 38amu. Fig. 9 shows the mass distribution spectrum with Gaussian fit.

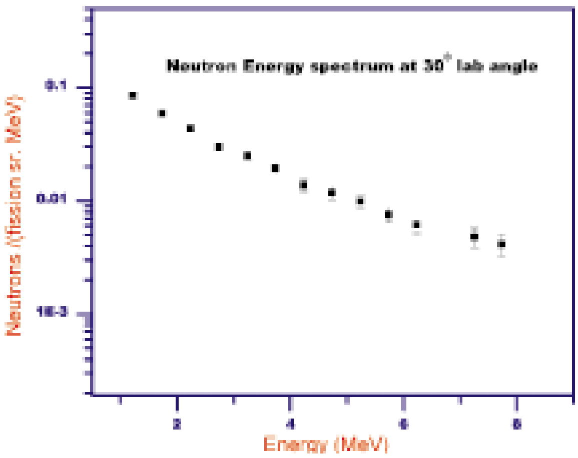

Fig. 8 : Neutron energy distribution

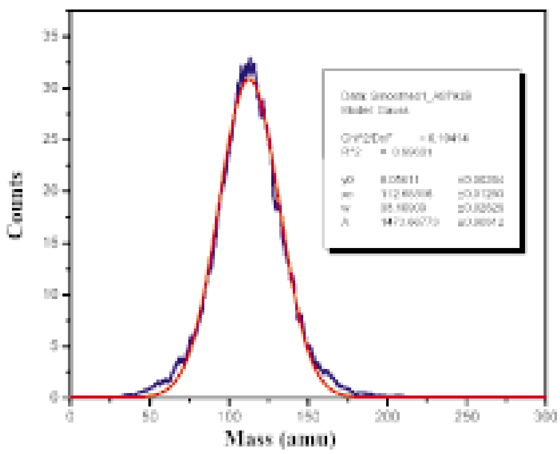

Fig. 9 : Mass distribution of fission fragments

4.1.7 Study on Complete and Incomplete Fusion Reactions

Dharmendra Singh[1], Afsal Ansari[1], Golda K.S[2]. Pankaj Kumar[2], P. Sugathan[2], S. Muralithar[2], R.K. Bhowmik[2]

[1]Aligarh Muslim University, Aligarh.
[2]Nuclear Science Centre, New Delhi-110067.

It is reported in seventies that the reactions induced by heavy ions like ^{12}C, ^{14}N, ^{16}O, etc leads to massive transfer into the target nucleus. These reactions compete with fusion reactions at energies near and above coulomb barrier. This incomplete momentum transfer, where some part of the projectile behaves as spectator while reminder fuses with the targets, are classified as incomplete fusion reaction. These reactions give rise to enhancement in fusion cross section than predicted by fusion models and it also shows a forward peaked angular distribution of out going particles. There are different approaches to study these reactions viz Recoil Range Distribution, Particle gamma coincidence measurements, angular distribution studies of charged particles. We had been studying these kinds of reactions using facilities at NSC, by adopting Recoil Range Distribution. To peep more deep into these kinds of reaction mechanisms, we have recently done an experiment using another approach, particle gamma coincidence technique.

The experiment is done with ^{16}O on 1mg/cm^2 thick ^{165}Ho target foil at 100 MeV. Two silicon surface barrier detectors at $\pm 11^0$; one above and one below the reaction plane, are used for beam flux normalization. Three ΔE-E telescopes at $\pm$ 30^0 and 54^0 are used for light charged particle detection. In these telescopes transmission detectors are of 40µm and stopping detectors are of 3mm/5mm thickness. The 30^0 telescopes have a solid angle coverage of 4.7msr and 5.3msr and the 54^0 telescope has a solid angle coverage of 1.07msr. A 100cc HPGe kept at 90° at a distance of 12 cm from the target is used for gamma ray detection. Fig. 10 gives the internal view of the scattering chamber showing telescopes, gamma detector re entrance cup, target ladder, etc. For data collection we demanded a two fold coincidence among the four parameters; three charged particle telescopes and one gamma ray detector. The energy calibrations of the telescopes are carried out with ^{241}Am alpha source and that of the high resolution Ge detector is done with ^{152}Eu source. Preamplifier signals from the ?E detectors are split and given to two amplifiers with different gain settings. The high gain amplifier is used for lighter particles like protons, alphas, etc. and the low gain amplifier for all the particles up to elastically scattered particles. Along with the energy information from all the detectors TAC is also

Fig. 10 : Internal view of the scattering chamber

generated between particle and gamma in order to distinguish prompt and delayed events. The signals are fed to 12bit ADC and the digitized data is collected using a CAMAC based multi-parameter data acquisition system for off-line analysis.

The data from the telescopes are transformed into two parameter maps of total energy versus energy loss, fig. 11. The energy distribution of the emitted particles are generated from these two dimensional plots. A typical energy distribution of alpha particles at 30^0 lab angle is shown in fig. 12. The energy spectrum for the prompt gamma rays is generated by gating the raw gamma spectrum with alpha particles detected by each telescope. But since the telescopes are seeing elastics most of the time, the genuine particle-gamma coincidence data collected is of very poor statistics. Hence any further studies cannot be carried out with the collected data. Still from this data we could draw the information about the typical energy distribution of the emitted light particles which can be used to determine upto what energy level the particle will be cutoff if an absorber is used to cutoff the elastics. Furthermore this experiment has given us a feeling about the cross section of light particle evaporation. These informations are valuable for better planning of similar experiments.

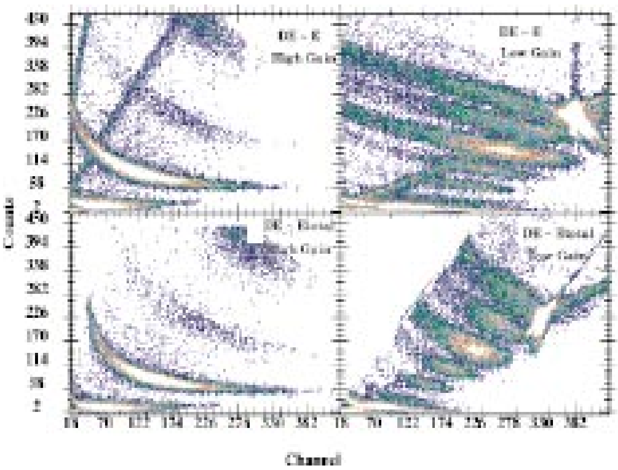

Fig. 11 : DE vs. E_{total} plots of 30° telescopes

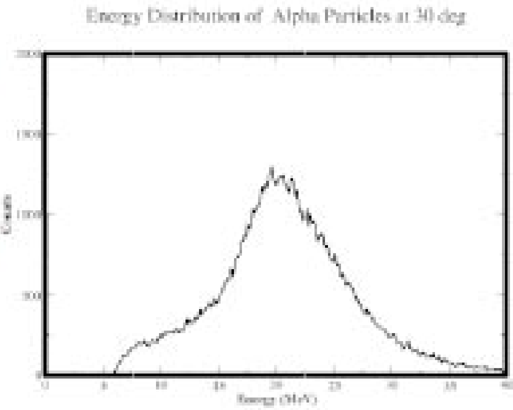

Fig.12 Energy distribution of emitted alpha particle

4.1.8 Compilation of Physics Codes

Sugathan. P and Golda. K.S

There are many different codes widely used by the physics user community. We have collected all the available physics codes, ported and compiled them under GNU/ Linux using Intel FORTRAN Compiler (IFC version 8) and GCC. The programs are now available from a server connected to the internal LAN. Sample input files and help files are provided for commonly used programs. For simple utility programs where large scale computation is not required, a user friendly web interface is also created. Programs like energy loss, charge state distribution, kinematics etc can be accessed by this interface. The user input is facilitated through web forms and the output is displayed on browser window. Figure below shows a typical web based interface for inputting the beam parameters to calculate the counts in monitor detectors. The programs can be accessed and run from anywhere using a browser window.

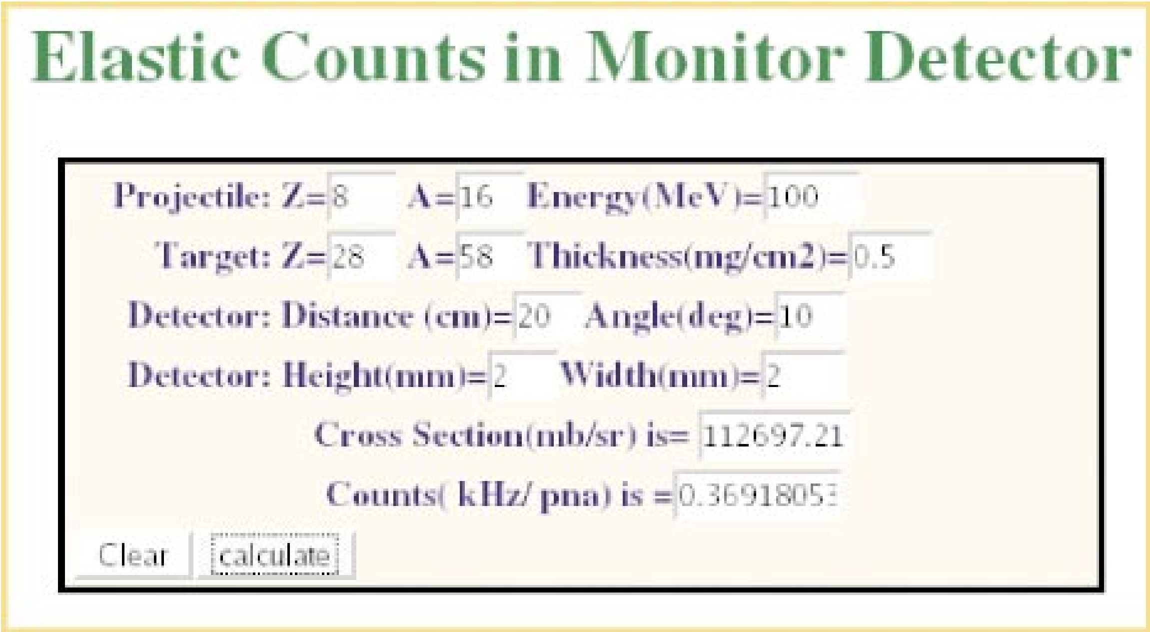

Fig. 5 : Web form based GUI to enter input parameters

4.2 GAMMA DETECTOR ARRAY (GDA)

Kusum Rani, Rakesh Kumar, S. Muralithar, R.P. Singh, and R.K. Bhowmik

The users of GDA facilities have published prolifically (8 nos.) this year (refer publication list). The activity in the GDA laboratory in this year was devoted in the following areas:

4.2.1 GDA resumption

After having Indian National Gamma Array at HIRA beamline in 2002-2003 the GDA electronics was moved to GDA beamline and reassembled so that we could conduct all the pending experiments of various users in GDA facility. This includes the Lifetime Measurement, Gamma Spectroscopy, and Perturbed Angular Distribution type of experiments.

4.2.2 Large Gamma detector Array (LGA)

The seed proposal of Large Gamma Array project was completed and completion report was submitted to Department of Science and technology. In this project, two numbers of Clover Germanium detectors and Anti-Compton shields, along with necessary High Voltage power supplies were procured. In this project many associated support equipments/software were developed:

- Multicrate Data Acquisition System with List Processor and Crate Controller – CANDLE,
- Offline analysis package – Ingasort,
- Clover Ge Electronics NIM modules which process 4 energy signals of Clover and
- Four time signals of Clover Germanium along with time signal from ACS,
- 8 K – 8 channel CAMAC ADC module,
- High Voltage Power supply for Ge detectors
- Automatic Liquid Nitrogen filling system.

4.2.3 Indian National Gamma Array

The support structure is modified to accommodate LEPS detectors (7 nos) also along with 24 Clover Germanium detectors with Anti-Compton Shields. The drawings of all parts are ready to place order for fabrication. The feasibility of fabrication is followed up with outside machine shops. The funds are awaited from Department of Science and Technology. The Electronics cum data acquisition cabin in Beamhall II is ready with 19” racks and laid out cable trays. After procurement of components the laying of beamline components/detectors/electronics will be taken up.

4.2.4 INGA at Kolkata

After extensive testing for reliability, linearity we sent ten number of NSC clover modules to VECC, Kolkata. They are used in ongoing experiments of Indian National Gamma Array at Kolkata. This has helped in reducing considerably the power, NIM bin space and interconnecting cables requirement besides reducing the tuning time. The electronics circuit used for collecting data at VECC, Kolkata INGA system is given below (Fig 1 & 2).

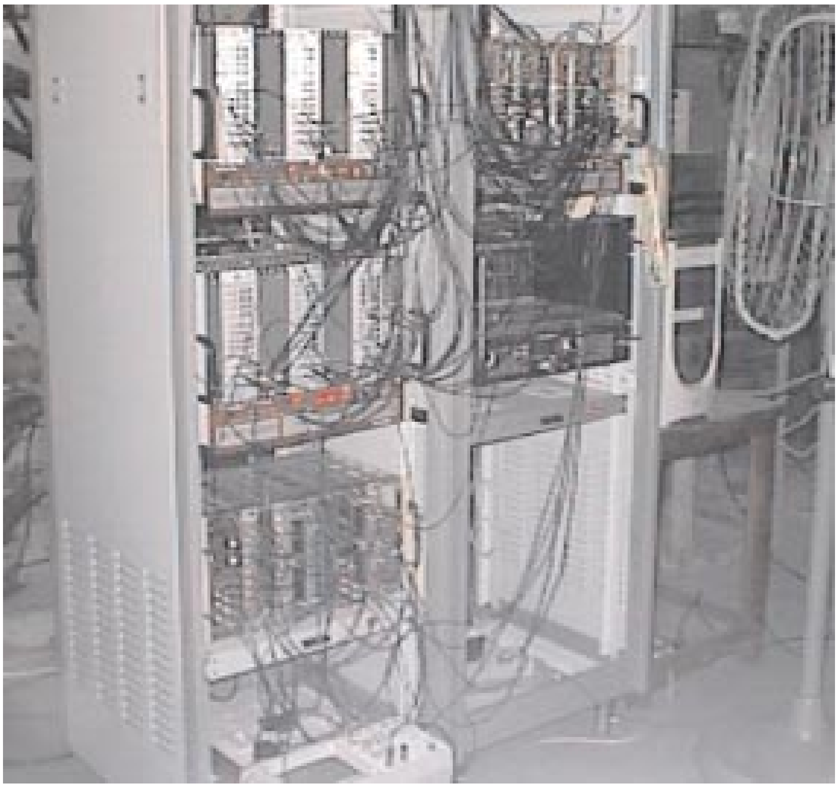

Fig. 1 : Electronics for INGA setup at VECC

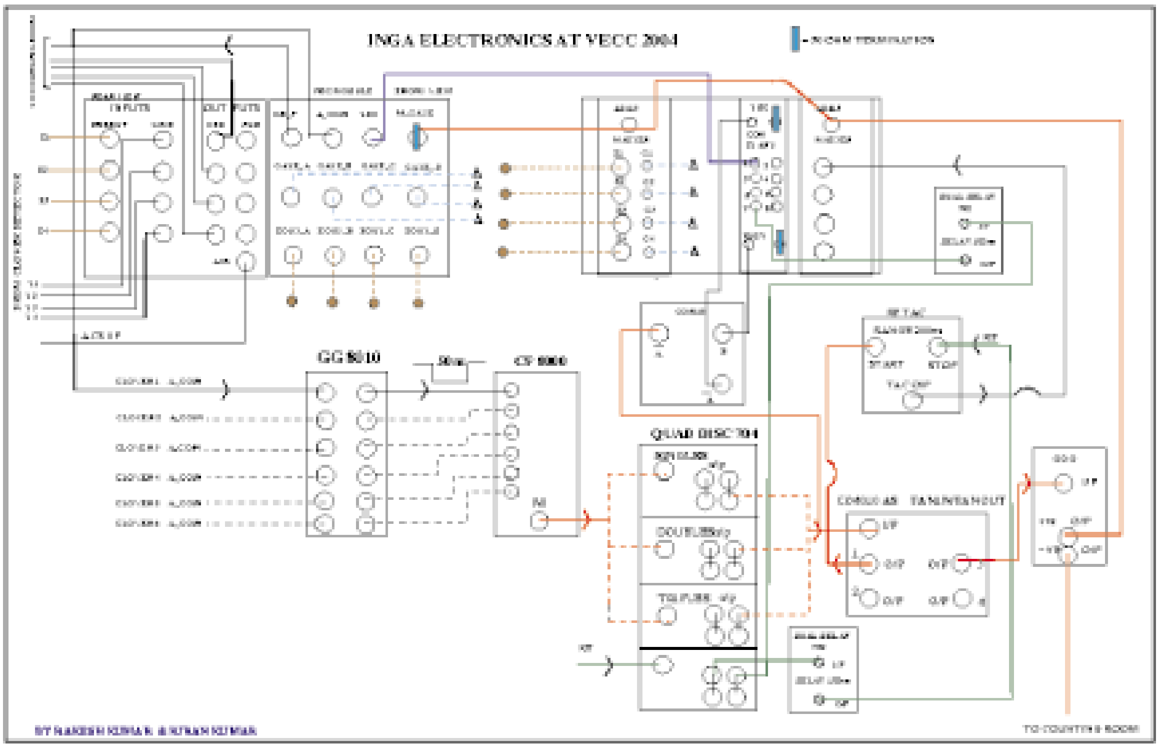

Fig. 2 : Block diagram for INGA electronics at VECC

4.2.5 Experiments

The GDA facilities were used very much in this year and the list of experiments is shown in the table below.

Description	Beam	Energy (MeV)	Shifts	User	Facility
Incomplete fusion in $^{16}O+^{165}Ho$	^{16}O	100	20	MAA/AMU	GPSC
HIRA + BGO Multiplicity filter	^{16}O	100	4	NM/NSC	Facility testing
Fusion time scale measurement	^{16}O	100	12	NMB/KU	HIRA + BGO Multiplicity filter
Entrance channel study in fusion reactions	^{16}O	76	11	GS/PU	GPSC
Fission Hindrance	^{16}O	84-124	4	NMB/KU	HIRA + BGO Multiplicity filter
Lifetime Measurements ^{167}Lu	^{16}O, ^{12}C	112 74	14	SKC/PU	RDM + GDA
Lifetime Measurements ^{134}La	^{15}N, ^{12}C	75	14	VK/IITM	RDM + GDA
Lifetime Measurements ^{132}La	^{15}N	86	12	VK/IITM	RDM + GDA
Magnetic Rotation by DSAM in Rb	^{19}F, ^{11}B	80, 50	12	PB/SINP	GDA
Shears Mechanism by DSAM ^{106}In	^{32}S	130	18	AD/BU	GDA
Quadrupole moment Measurement in ^{175}Ta	^{19}F	87	6	AKB/PU	PAD
Shears Mechanism by DSAM A ~ 110	^{30}Si	120	17	AD/BU	GDA
Lifetime in Magnetic Rotation – $^{195,197}Pb$	^{16}O	97	8	SCP/DU	GDA, Pulsed beam
Quadrupole moment Measurement in $^{170,171,172}Hf$	^{16}O	78-104	8	AKB/PU	PAD, Pulsed beam
Nuclear structures by DSAM	^{27}Al	120	22	LC/BHU	GDA
Structure in N~86	^{14}N	70	18	AG/SINP	GDA

4.2.6 Nuclear Physics with LINAC beams at NSC

A workshop on Nuclear Physics with LINAC beams at NSC was held on 17th September 2004 at NSC. About 35 participants came from different universities, colleges, and Institutes. The workshop was in group discussion format which was basically addressed the physics experiments which could be taken up with the Beam hall II facilities like INGA, HYRA, GPSC, Neutron Array, CPDA and with LINAC beams.

4.3 RECOIL MASS SPECTROMETERS

4.3.1 Heavy Ion Reaction Analyzer (HIRA)

Subir Nath, Akhil Jhingan, Thomas Varughese, J.J. Das*, P. Sugathan, N. Madhavan, P.D. Shidling[1]

*On leave, at ORNL (USA)
[1]Department of Physics, Karnatak University, Dharwad, Karnataka

After a series of experiments with HIRA + INGA combination and a few experiments using ^{7}Be RIB in the preceding two years, HIRA was again operated in the mass dispersion mode for the selection of fusion evaporation residues from a very heavy system (^{200}Pb compound nucleus). HIRA worked well and data could be taken as per plans for this system which is one of the heaviest systems accessed using HIRA. The experiment looking for fission hindrance in ^{16}O + ^{184}W $\rightarrow$ ^{200}Pb* was carried out with HIRA + 14 BGO detectors. Sliding seal chamber with PHOPDISC assembly was used for this purpose with a charge state reset foil beyond the target at ~ 10 cm distance. Enriched ^{184}W target (~ 200 μg/cm^2) on Carbon backing (~ 100 μg/cm^2), prepared at NSC, was used in the experiment. The focal plane detector, a large 2D SB detector (as the residues were of less energy, ~ 7 MeV), along with the time-of-flight signal helped in getting rid of beam related background event and to select only the evaporation residues. Pulsed beam with 4 microsecond time interval between pulses (by the use of TWD) was used as the residues had a flight time through HIRA of ~ 3.5 microseconds. Details of the experimental set up are discussed in section 5.

In maintenance side, all the water-cooled, transistor heat sinks in the five high current, magnet power supplies were replaced mostly by indigenously developed heat sinks. This had to be done on priority basis as the original heat sinks were developing leaks due to corrosion. Leaks in the heat exchanger in quadrupole power supply have been rectified. The ED cryo compressor, which developed a water leak in the heat exchange unit, was replaced by a spare compressor and placed at a comfortable location on a newly designed trolley fixed to the HIRA platform.

The gap between HIRA facility and zero degree beam-line was plugged by radiation shielding wall. The far end of the existing shielded portion was further strengthened by 30 cm brick wall which should allow the use of proton beam in HIRA facility without affecting the work in Phase II (LINAC) vault.

4.3.2 HYbrid Recoil mass Analyzer (HYRA)

N. Madhavan, S. Nath, P. Sugathan, J.J. Das*, A. Jhingan, T. Varughese, A.K. Sinha[1], R. Singh[2], K.M. Varier[3], M.C. Radhakrishna[4], Cryogenics Group and Beam Transport Group.

*On leave, at ORNL, USA
[1]IUC-DAE Consortium for Scientific Research, Kolkata Centre, Kolkata
[2]Department of Physics and Astrophysics, University of Delhi, Delhi
[3]Department of Physics, Calicut University, Kerala
[4]Department of Physics, Bangalore University, Bangalore

Detailed design of the ion-optical components of most of first stage of HYRA (see figure 1), the associated chambers, support structures, movement mechanism, etc. have been worked out through communication with the supplier (M/s. Danfysik, Denmark). Two NSC personnel took part in the design finalisation meeting at Danfysik. The drawings/ parameters have been checked and corrected as per requirements and finalised, based on three dimensional field calculations for various dipole and quadrupole magnets. The design layout is shown in fig 2. Special care has been taken for beam dump in first magnetic dipole for both gas-filled mode (where beam gets bent more than the residues) and vacuum mode (where beam gets bent less than the residues) by the design of Tantalum linings with water-cooled copper backing. A Faraday cup/beam stopper is planned which can be inserted in the straight through port of MD1 to stop the beam if magnetic field is turned off accidentally.

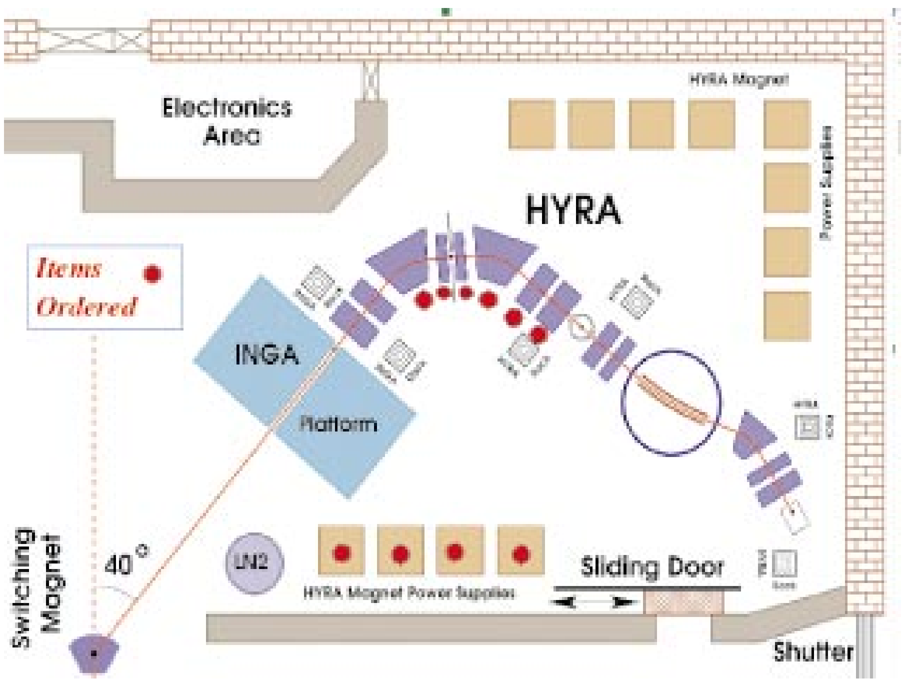

Fig. 1 : The layout of HYRA highlighting the components ordered or developed.

Fig. 2 : 3D model of MD1-Q3-MD2 (with chambers, support structures and movement mechanism) of first stage of HYRA

The fabrication of magnets for most part of first stage of HYRA is over (see figures 3 and 4) and detailed field tests are being carried out in the presence of two scientists from NSC. The equipments are expected to be shipped on successful completion of these tests and acceptance by NSC. The installation of these components is expected to start in the middle of this year.

The first quadrupole doublet Q1 and Q2, which are planned to be of “super-ferric”, superconducting type for increased angular acceptances, is being designed. Two members from the Cryogenics group visited MSU to interact with experienced personnel in this field. The components will be procured and fabrication of various parts along with those of second stage will begin with the release of next instalment of money from DST.

The work on the focal plane detector systems for the two modes of HYRA have begun and large area gas detectors will be adapted to HYRA. The detector for residue and alpha decay detection (strip detector) has been procured and will be used with discrete and custom-made electronics. A clock module, developed at NSC, will be used for time correlation between arrival of residues and the successive alpha decays to identify the A and Z of the residue in gas-filled mode. This detector will be preceded by a large area MWPC for TOF estimate to differentiate between residues and target-like particles and to differentiate between residues and alpha particles detected in strip detector when the energies are comparable.

Fig. 3 : Split quadrupole Q3 of HYRA.

Fig. 4 Magnetic dipole MD1 of HYRA.

A one day workshop was held in September 2004 ("Nuclear physics with LINAC beams at NSC"). Parallel sessions were held in identified areas to initiate working group formation and ideas for group experiments. This was followed by HYRA investigators' meeting at NSC. The design and plans related to HYRA were presented in an invited talk in DAE-BRNS Symposium on Nuclear Physics, 2004 at BHU.

The indigenous power supply (300 A, 100 V) components are being mounted in a single cabinet designed for this purpose. Work has started for the design of power supplies for the four quadrupoles of second stage of HYRA.

The Phase II beam hall radiation shielding in the Nuclear Physics beam-line is almost complete. An opening is provided for movement of large and heavy magnets into the hall. The electronics cabin has been made and racks and cable trays are in place. The utilities such as electrical power and cooling water distribution network are designed and installation work has commenced.

4.3.3 Transmission Efficiency of Recoil Separators

S. Nath and N. Madhavan

A common use of recoil separators is the efficient separation of rare evaporation residues (ERs) from the intense primary beam at forward angles (around 0^o). ERs are separated, transported and detected in a background-free focal plane area. Trajectories of the ERs are governed by the electric and magnetic fields of the separator. Transmission efficiency of ERs through a recoil separator is often a very useful quantity in planning an experiment and analysing data. Standard ion-optical programs e.g. GIOS [1] are used to simulate the motion of ERs in the separator. However, these codes are not suitable to extract the *realistic* transmission efficiency of ERs through the separator, mainly because the average values of energy, angle and charge state are considered. Any reliable calculation of transmission efficiency must include realistic distributions of the above mentioned quantities taking particle evaporation and target thickness effects into account.

We report a simulation program, based on Monte Carlo technique, for calculation of ER transmission efficiency in recoil separators. In this program *real* ERs are generated event-by-event and transported through the separator. Trajectory of each ER is subjected to a number of checks dictated by the acceptance and hardware limitations of the separator. The ratio of the ERs *surviving these checks and completing their journey up to the detector* to the total number of ERs *generated* is a measure of the transmission efficiency. The program is written in C language and has two distinct parts, as described below.

(i) Interaction at target site

Interactions of beam particles with target nuclei are treated in a semi-microscopic way [2, 3]. The *fusion-point* is chosen randomly inside the depth of the target foil. Energy loss of beam up to this point and that for the ER in the remaining thickness of the target is calculated [4]. Particles (neutron, protron and α, based on user input) are sequentially *evaporated* isotropically in the centre of mass frame with energies characteristic of the nuclear temperature at available excitation energy. Energy spectra of the evaporated particles follow Maxwellian distribution. The recoil-kicks imparted to the ERs by the particles give rise to angular distribution of the ERs. Change in ER energy because of momentum conservation is also taken care of. Finally a charge-state is assigned to each ER, using empirical formulae for charge state distribution [5, 6]. Energy, angle and charge-state of the given number of ERs, thus calculated, are stored. The x, y positions of the ERs w.r.t. the beam axis are chosen randomly within a given spot size of the accelerated beam. These values are used as inputs to the next part of the program.

(ii) Trajectory calculation

Each ER starts its journey from the target to the detector with the following set of values : x, θ, y, ϕ, m, E and q (in conventional ion-optical notation). Trajectory of each ER is calculated by first order transfer matrix method [7]. Apertures are *placed* at appropriate locations along the beam axis conforming with the hardware design of the separator. Dimension of the detector is also taken care of. Only those ERs, which complete their journey up to the detector, contribute to the transmission efficiency of the separator. For adapting the program for a particular recoil separator, only this part of the program needs to be modified.

The program has been used to calculate ER transmission efficiency through HIRA [8], for a few systems. The results are shown in Table. I and found to be matching closely with the measured values (wherever available). Energy spectrum of evaporated neutrons (fig. 1), ER angular (fig. 2), energy (fig. 3) and charge state distributions (fig. 4) and ER trajectories through HIRA in dispersive (fig. 5) and non-dispersive planes (fig. 6) are shown for the system ^{175}Lu(^{19}F, 6n)^{188}Hg at beam energy 119.1 MeV.

Currently we are engaged in incorporating the effect of multiple scattering in the target on ER angular distribution (especially for thicker targets). Based upon the encouraging results obtained for HIRA, we are also adapting this program for the vacuum mode operation of HYRA [9] spectrometer, being built at NSC, funded by Department of Science and Technology, Government of India. In future, we plan to extend this program to simulate transmission efficiency of gas-filled mode of HYRA.

REFERENCES:

[1] H. Wollnik et al., Nucl. Instr. and Meth. A258 (1987) 408.

[2] A.G. Popeko et al., Nucl. Instr. and Meth. B126 (1997) 294.

[3] A. Marozin et al., Nucl. Instr. and Meth. B126 (1997) 290.

[4] A.F. Ziegler et al., The Stopping and Range of Ions in Solids, Pergamon Press, New York (1985).

[5] V.S. Nikolaev et al., Phys. Lett. A28 (1968) 277.

[6] R.N. Sagaidak et al., Nucl. Instr. and Meth. B93 (1994) 103.

[7] H. Wollnik, The Optics of Charged Particles, Academic Press, New York (1987).

[8] A.K. Sinha et al., Nucl. Instr. and Meth. A339 (1994) 543.

[9] http://www.nsc.ernet.in/research/nuclear_physics/index.html.

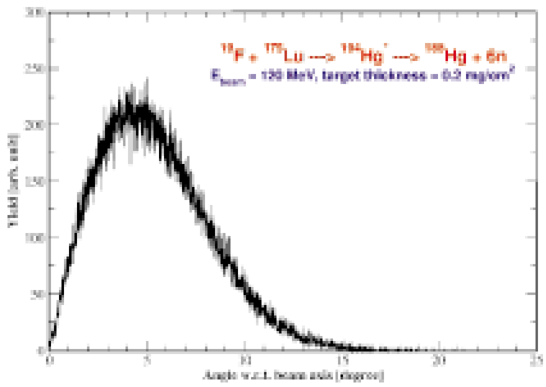

Fig. 1 : Evaporated neutron energy spectrum

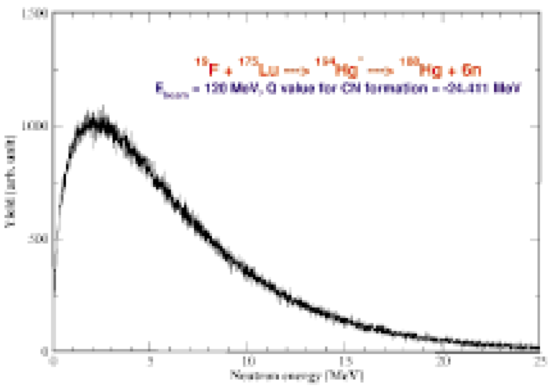

Fig. 2 : ER angular distribution

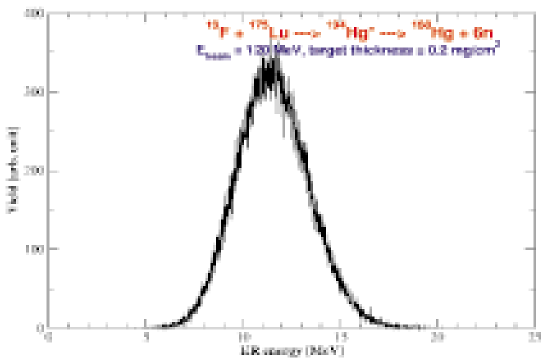

Fig. 3 : ER energy spectrum

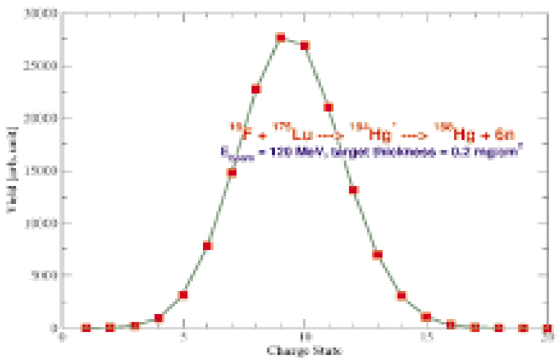

Fig. 4 : ER charge state distribution

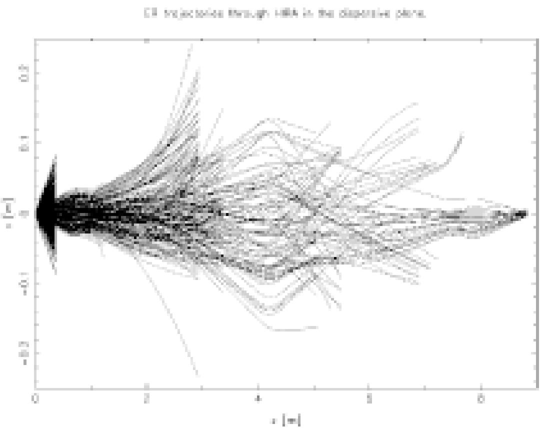

Fig. 5 : ER trajectories through HIRA in the dispersive plane.

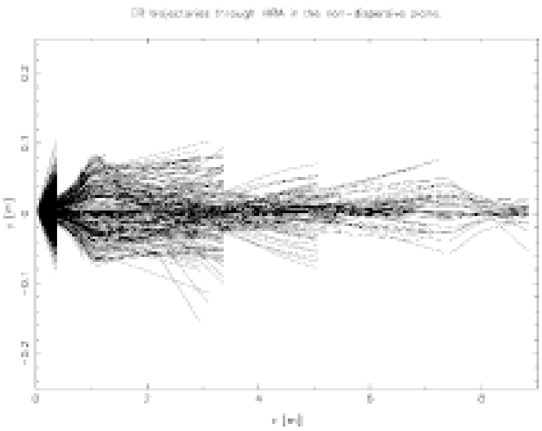

Fig. 6 : ER trajectories through HIRA in the non-dispersive plane.

Table I. Calculated ER transmission efficiencies through HIRA

System	Beam energy [MeV]	Q value [MeV]	Target thickness [mg/cm^2]	Solid angle [msr]	Transmission Efficiency [%]
$^{184}W(^{16}O, 4n)^{196}Pb$	83.6				1.8
$^{184}W(^{16}O, 5n)^{195}Pb$	91.6				1.1
$^{184}W(^{16}O, 5n)^{195}Pb$	99.6	-24.19	0.21	10	1.3
$^{184}W(^{16}O, 6n)^{194}Pb$	107.6				1.2
$^{184}W(^{16}O, 6n)^{194}Pb$	115.6				1.4
$^{184}W(^{16}O, 7n)^{193}Pb$	123.7				1.3
$^{175}Lu(^{19}F, 4n)^{190}Hg$	88.9				3.5
$^{175}Lu(^{19}F, 5n)^{189}Hg$	97				2.8
$^{175}Lu(^{19}F, 6n)^{188}Hg$	109	-24.41	0.2	10	2.2
$^{175}Lu(^{19}F, 6n)^{188}Hg$	119.1				2.4
$^{175}Lu(^{19}F, 7n)^{187}Hg$	129.2				2
$^{175}Lu(^{19}F, 8n)^{186}Hg$	138.2				1.8
$^{93}Nb(^{19}F, 3n)^{109}Sn$	58	-0.04	0.44	5	2.4
$^{64}Ni(^{46}Ti, 3n)^{107}Sn$	135	-25.39	0.24	5	11.2
$^{60}Ni(^{50}Ti, 3n)^{107}Sn$	145	-30.06	0.27	5	13.5
$^{58}Ni(^{28}Si, 2n)^{84}Mo$	92	-16.72	0.45	5	7.1
$^{27}Al(^{32}S, 3pn)^{55}Fe$	110	13.14	0.2	5	3.6
$^{12}C(^{32}S, 2pn)^{41}Ca$	110	11.53	0.2	5	7.1
$^{12}C(^{28}Si, pn)^{38}K$	88	13.35	0.1	5	8.4

4.4 MATERIALS SCIENCE FACILITY

A. Tripathi, Ravi Kumar, V.V. Shivkumar, F. Singh, S.A. Khan, P. K. Kulriya, T. Mohanty, D. Kabiraj, R.N. Dutt, P. Barua, A. Kothari, D. Kanjilal and D.K. Avasthi

The materials science facilities continue to support the research programmes of a large number of users from different universities and institutions from India and abroad. The swift heavy ion irradiation related experiments are performed in the three chambers in the beamline as well as in the general purpose scattering chamber. Besides this the off-line facilities are also being used by many users for preparing and characterizing samples. A total of 85 user experiments comprising more than 200 shifts were performed this year, without any beam time loss due to any major facility break down. Special emphasis is being given to thrust areas where group experiments are being conducted. Experiments are being done in different areas of swift heavy ion induced materials modification and characterization and the details of the research programmes are given in Section 5.2.

The high vacuum chamber in materials science beamline is used in most of the experiments. A 1000 l/s Turbo pump from Pfeiffer has been installed in place of 500 l/sec turbo pump to reduce the pump down time for pumping the chamber. A quadrupole mass analyser with SIMS option has been integrated to UHV chamber.

FTIR system Nexus 670 from Nicolet is being actively used for vibrational analysis of thin films as well as bulk materials of various users. Nearly 250 samples have been analyzed. The PL/IL studies of more than 400 samples from nearly 30 users have been carried out during this year.

4.4.1 Sample ladder for irradiation chamber in beamhall II

A. Tripathi and R. Ahuja

The installation of the beamline in the Beam hall II up to the irradiation chamber was completed last year. The irradiation chamber with a sample ladder to mount 4 samples for testing was also installed. The new target ladder for irradiation chamber in Beam Hall II was designed and fabricated this year. The six sided ladder has provision for mounting 8 samples (1 cm x 1 cm) on each side. Three sides have 10 mm x 10 mm x 1 mm slots provided for mounting samples with metal clips. The ladder has provision for cooling samples down to liquid nitrogen temperature. Three 10 pin current feedthroughs have also been provided for transport measurement studies. Fig 1 shows a photograph of the ladder.

Fig. 1 : Sample ladder for irradiation chamber in beam hall II.

4.4.2 Sample ladder linear and rotational motion

A. Tripathi, R.N. Dutt and S.A. Khan

Linear motion and rotary table for the sample ladder have been acquired and plans for computer controlled remote operation are underway. Computer control for Z motion and rotary motion is based on Windows platform. Methods to introduce limit switches for Z motion are being worked out presently. Software is tested successfully with the offline test setup. It will also support limit switches as soon as they are ready. The indexer/controller system, which had a minor manufacturing defect, has arrived recently after warranty repair from MDC and the final system along with the limit switches etc is underway.

4.4.3 Plasma based deposition of thin films

V.V. Siva Kumar and D.K. Avasthi.

The primary objective of plasma based thin film deposition work at NSC is to synthesize thin films for users. To work with wider variety of materials, regular upgradation of rf sputtering system is taken up and development of microwave plasma based CVD system is underway.

4.4.3.1 RF sputtering system

V.V. Siva Kumar

The RF sputtering system is operational for thin film deposition. This year problems were encountered with the RF power supply, chamber vacuum and high vacuum production, which were solved. The system was also used for testing of the developed matching network and RF power supply. The circuit for rf self bias that develops on the target during deposition, was calibrated using the 4 inch diameter target holder. Thin film deposition from the following targets was undertaken during this period: Zinc oxide (BRS college, Agra), Ni-Ferrite and Mg-Mn Ferrites (HPU), FeNiBMo4 (CU, Kerala), and Ge/SiO2 (IITD). Deposition of films from ferrite target with diameter much less than 50 mm, using 2 inch dia target holder gives problems related to plasma production.

A set-up to deposit thin film multilayers is being developed. It will have two magnetron target holders for 2 inch dia targets and substrate holder with provision for rotation. Provision is made for users to learn the operation of rf sputtering system for depositing films using a 100 mm dia copper target.

4.4.3.2 Development of microwave CVD deposition system

V.V. Siva Kumar, P. Barua, R. Ahuja, S. Rao and D.K. Avasthi

The microwave components for the microwave plasma based thin film system were procured from M/s Richardson Electronics, USA. The deposition chamber was leak tested. The leaks were rectified and the chamber was tested for vacuum. Assembling the system for testing and thin film deposition by CVD using C_2H_6 gas, will be undertaken this year in the new materials science building. Feasibility study of sputtering using ions from the microwave plasma and upgrading the microwave plasma system to ECR plasma system, has been planned.

4.4.3.3 Growth of ZnO nanocrystals in silica by rf co-sputter deposition and post-annealing

V.V. Siva Kumar, F. Singh, Amit Kumar and D.K. Avasthi.

Growth of ZnO nanocrystals in silica matrix is being studied using different deposition and annealing conditions. Thin films were deposited from a pure Si target (100 mm dia), pure ZnO target (50 mm dia) and a composite ZnO/Si target prepared by pasting ZnO pellets to the Si target. Thin films deposition from ZnO/Si target was done at different process pressures, rf powers, substrate temperatures (between 350^{o}C and 750^{o}C), time durations and with different sizes of ZnO pellets. Post annealing was done in air/ high vacuum at different temperatures ranging from 350^{o}C to 1000^{o}C.

UV-VIS and Photoluminescence spectra of the films show blue shift in band edge and visible luminescence peak for the ZnO nanostructures grown in silica in the deposited ZnOSiOx film which suggest growth of ZnO quantum dots in silica. Characterization and analysis of other films is under progress.

4.4.4 Ball Milling system for synthesis of nanopowders

V.V. Siva Kumar and Ravi Kumar.

The ball milling system was used to synthesize nanocrystalline ferrite powders for user of Andhra University. Four powder samples with change in dopant concentration were milled for 5 hours with a ball to powder ratio of 10:1.

4.4.5 Swift Heavy Ions in Materials Engineering and Characterization (SHIMEC)

D.K. Avasthi, A. Tripathi, Ravi Kumar, F. Singh, S.A. Khan and P. K. Kulriya

The SHIMEC programme has been funded by DST under its Intensifying Research in High Priority Areas (IRPHA) programme. The thrust areas identified under the project are the study of Phase transformation, Electronic/ Potential Sputtering, Surface/Interface modification, Ion beam induced epitaxial crystallization, Nano phase modification and synthesis and Transient-enhanced diffusion. The following instruments have been installed under the project:

4.4.5.1 Scanning Probe Microscope

A. Tripathi, S.A. Khan and V. Baranwal[1]

[1] University of Allahabad

Multi Mode SPM with Nanoscope IIIa controller acquired from Digital/Veeco Instruments Inc. has been installed and the following modes of operation have been used in user experiments: Contact/ Tapping Atomic force microscopy, Scanning tunneling microscopy (STM), Magnetic force microscopy (MFM) and conducting AFM . The areas of research include: Ion induced surface morphology, SHI induced changes in size and its distribution of nanoparticles, SHI induced modification in magnetic domains, SHI induced plastic flow of material and Characterization of ion tracks in terms of size and number density. This system is actively being used by users and more than 200 samples from 40 users have been studied. Three of the illustrative images taken in Tapping mode AFM (Fig1), MFM (Fig 2) and C-AFM mode (Fig 3) are shown below and results obtained are discussed in materials science research section 5.2.

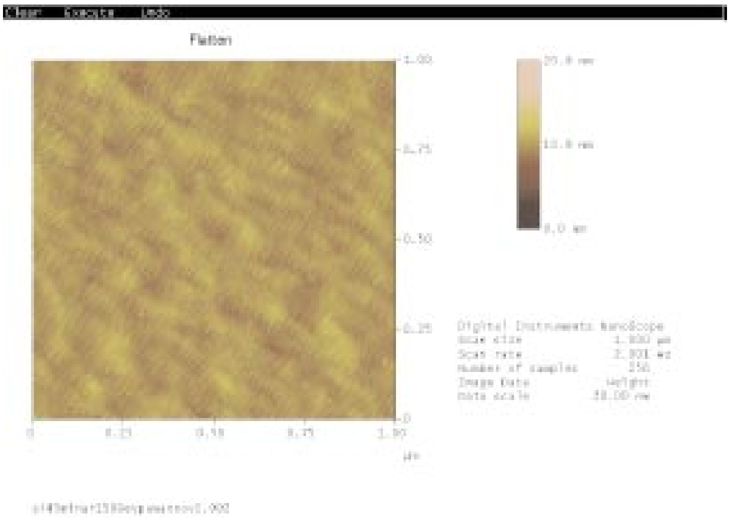

Fig. 1 : 1.5 KeV Ar beam induced ripple formation on Si surface by Tapping AFM

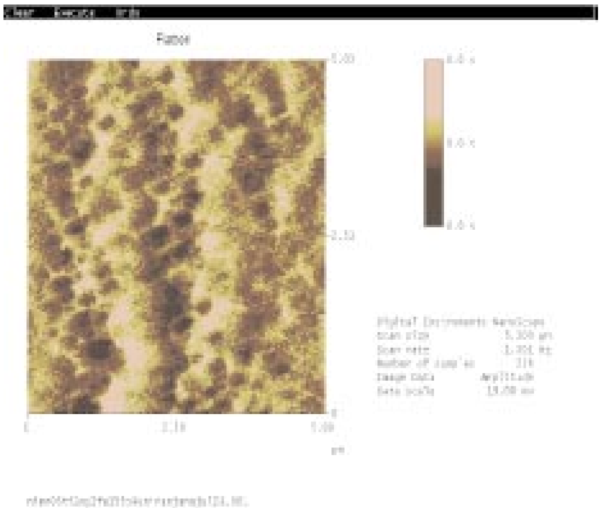

Fig. 2 : Magnetic domains in NiMnTiMgFeO films by MFM

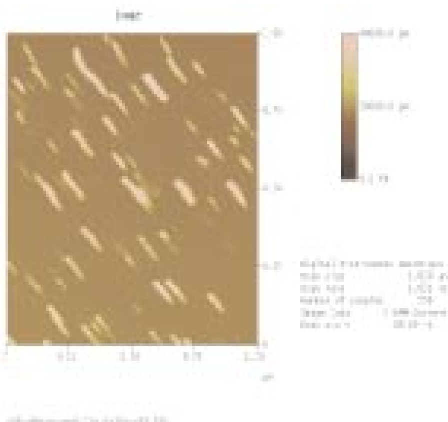

Fig. 3 : Conducting tracks in fullerene films by Conducting AFM

4.4.5.2 In-situ XRD set up

F. Singh, A. Kothari, R. Ahuja, P. Kulriya, A. Dogra, Y. Katharria and D.K. Avasthi

It consists of a 3 kW X-rays source with multi-layer mirror and will have the thin film attachment. This system is installed in the beamhall.

XRD (Model D8 Advance) has been acquired from Bruker AXS Germany, and offline testing has been completed. The system consists of a 3 kW X-rays source with multi-layer mirror and will have the thin film attachment. This system is installed in the beamhall and will be used for structural studies in the following areas: Novel phase formation, Phase transformations, SHI induced changes in size of nano particles and Surface and interface modification using XRR mode. X-ray diffraction technique is highly used structural characterization for materials modifications under SHI irradiation. Irradiation leads to amorphization, crystallization and phase transitions which depend on the irradiation parameters. In light of this requirement, we have designed and developed in-situ XRD facility in beam hall, and ex-situ testing were done and in-situ testing has to be done. This XRD is a versatile in nature like it could be used in different modes as follows;

Powder diffraction mode with spinning of sample
Glancing angle XRD for thin film applications
X-ray reflectivity for thin film and multi-layers characterizations

The facility is also equipped with a high speed position sensitive detector besides conventional NaI(Tl) scintillation counter. Its is about 60 times faster as compared to scintillation counter with reasonably good resolution. This detector will be very useful for in-situ ion irradiation experiments, where fast scanning is required to optimize the utilization of accelerator time. Setup as shown in Fig 1 is well aligned and calibrated using Corrundum and spectra of many samples were recorded in powder and glancing angle modes.

Fig. 1 : D8 XRD system with the irradiation chamber in Beamhall II

The fitted and Retweld refined XRD spectra of a ferrite sample, which was synthesized at NSC using solid state reaction technique is shown in Fig 2a. The spectra of pristine and irradiated C_{60} samples is also shown in Fig 2b. This data is also fitted and analysis is in progress.

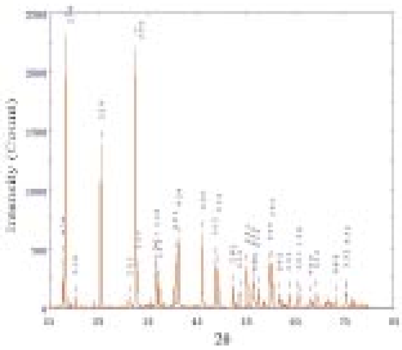

Fig. 2a : XRD spectra of a ferrite sample

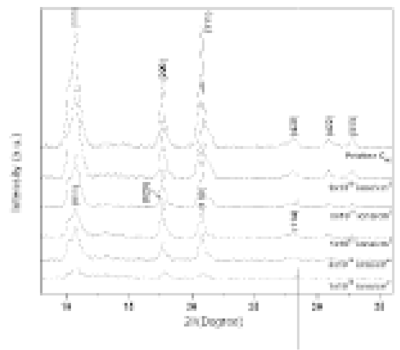

Fig. 2b : XRD spectra of a C_{60} sample

4.4.5.3 On-line QMA/RGA system

A. Tripathi, S.A. Khan and P. Barua

The Pfeiffer QMA 422 quadrupole mass analyzer system with SIMS option for mass range 1-1024 amu has been installed (Fig 1) . The QMA has a 3 lens optics for detecting both positive and negative ions as well as neutral atoms. The facility will be used for on line detection of release of gases, specially from polymers and online study of electronic sputtering.

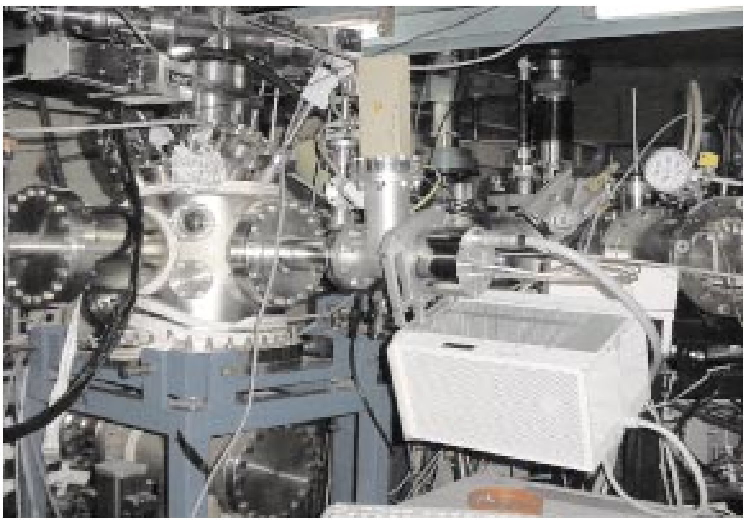

Fig. 1 : Pfeiffer QMA 422 quadrupole mass analyzer system with SIMS option

The facility has been tested offline and sample spectrum showing sputtered Au is shown in Figure 2.

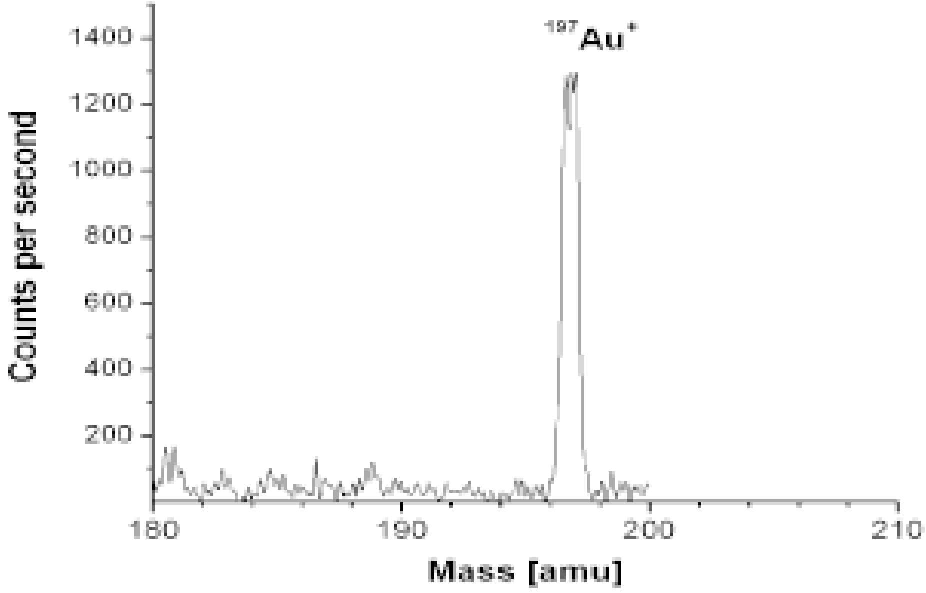

Fig. 2 : Spectrum showing sputtered Au with bombardment of 5 keV Ar beam.

4.4.5.4 Testing and usage of a new large area position sensitive detector telescope

S.A. Khan, M. Kumar[1], V. Baranwal[1], D.C. Agarwal[2], S. Kumar[2] and D.K. Avasthi

[1]University of Allahabad, Allahabad-211002
[2]R. B. S. College, Agra-282002

A recently fabricated large area position sensitive gaseous detector telescope [1] was tested and subsequently used in some of the experiments for on-line measurement of SHI induced compositional changes.

The detector is fixed to a 45° port of the high vacuum chamber of materials science beam line. The detector offers good Z resolution as shown in Fig. 1(a) which shows a bi-dimensional ΔE-E recoil spectrum recorded for a silicon oxy-nitride sample. The ΔE_1 signal discriminates very well between the recoils of adjacent masses like C, N, O as in this example. The two dimensional position spectra recorded during facility test using 120 MeV Ag ions is shown in Fig. 1(b). The position sensitivity in scattering plane is around 0.1 which is good enough for correcting the kinematic broadening of the detector (~17% in the present ERD geometry due to the large acceptance of the detector).

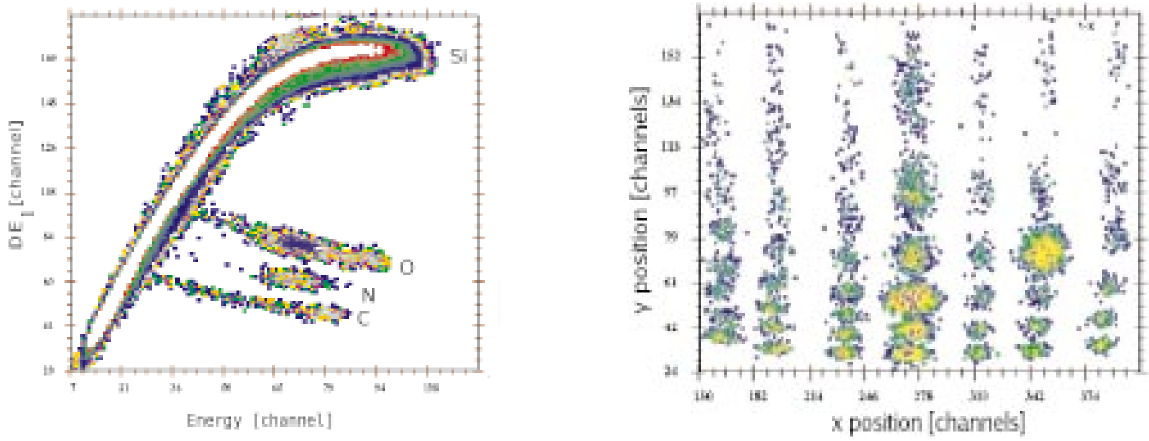

Fig. 1(a) Two-dimensional ΔE_1-E spectrum of recoils from O and N implanted silicon wafer. The spectrum was obtained using 60 MeV Ni^{5+} projectiles. (b) The xy-position spectrum of fluorine recoils entering the detector after passing through a mask consisting of 49 holes arranged in 7 rows and 7 columns. Two of these holes (one each in 4^{th} and 6^{th} columns) are of 3 mm diameter, remaining holes in 4^{th} column are of 2mm diameter while others are of 1 mm diameter. The separation between two rows/columns is 5 mm.

The detector has been frequently used in ERDA experiments to monitor swift heavy ion induced modifications like electronic sputtering, ion beam mixing and loss of volatile components (e.g. N) of the sample. A recoil spectra recorded during sputtering studies from 150nm thick film of LiF on Si substrate is shown in Fig. 2. Details of this sputtering measurement performed using 120 MeV Ag ions has been presented elsewhere[2]. The width of the peaks are related to the thickness of the film. As is evident from the figure, the thickness reduces with fluence due to sputtering. At higher fluences there is a signature of ion beam mixing as indicated by the change in slope of the lower energy part of the peaks as in the curve (c) of Fig. 2.

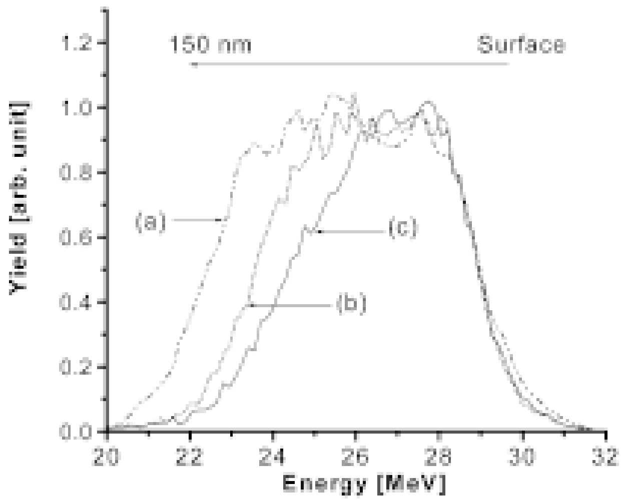

Fig. 2 Fluorine recoil spectra of (a) Pristine sample, (b) sample after fluence of 4.3×10^{13} ions/cm^2 and (c) sample after fluence of 2×10^{14} ions/cm^2.

REFERENCES

[1] S. A. Khan, M. Kumar, D. K. Avasthi, A. Jhingan, A. Tripathi, A. C. Pandey, NSC Annual Report (2003-04) 89.

[2] M. Kumar, S. A. Khan, F. Singh, A. Tripathi, D. K. Avasthi, A. C. Pandey, Indo-German workshop on synthesis and modification of nano-structured materials with energetic ion beams, New Delhi, 20-24th February, 2005.

4.5 ATOMIC PHYICS BEAM LINE

4.5.1 Status of Atomic Physics Beam Line

P. Barua, R. Ram, A. Kothari, Nissar Ahmad, Ranjeet Karn and T. Nandi

There was some re-shuffling of the beam lines last year. AMS beam line was dedicated in the LIBR and Atomic Physics line was dismantled for shifting to beam hall II. As of now the atomic physics scattering chamber has been reinstalled in the line. It has been anchored to the floor with a new mechanism keeping provision of aligning the chamber also. Inclined and straight electrostatic analyzer is also put in place. Multiple target holding ladder is now shifted from top flange to the bottom and x-ray photon normalization is being tried to have reliable data by a gas absorption cell instead of making use of Si-surface barrier detectors.

A Doppler Tuned Spectrometer is being developed indigenously. It will be installed in the GPSC chamber. Details are given below in section 4.5.2.

4.5.2 Development of DTS Setup in GPSC

Ranjeet Karn, Nissar Ahmad[1], R. Ram, and T. Nandi

[1]Dept. of Physics, AMU, Aligarh

High precision spectroscopy of highly charged ions (HCI) provides a powerful tool for exploring relativistic and quantum electrodynamics effects. Study of HCI may thus open up a hitherto unexplored realm of physics, shedding light on many astrophysical and quantum electrodynamics mysteries. Beam foil time of flight technique serves as a versatile tool to measure the lifetime of different energy levels, which can be applied in principle to any charge state. However, this technique does suffer from inherent cascading and blending problems. In order to get rid of satellite blending problem, people are developing high resolution spectroscopy. Doppler Tuned Spectroscopy (DTS) is one of the most elegant tools to achieve such a high resolution.

In most beam-foil experiment, the Doppler Effect produces unwanted distortion of emission spectra obscuring important features by extreme broadening. This broadening can be reduced by narrowing the acceptance aperture. However, Doppler Tuned Spectroscopy makes use of said Doppler Effect as a dispersive element. In this method, dispersion is due to variable Doppler shift vs angle of emission from the beam.

If an x-ray photon of energy E_0 is emitted at an angle θ by an ion beam (source) moving with velocity v, then one observes a shifted energy E_{ab} which is given by

$$E_{ab} = \gamma\,[1- (v/c)\cos\theta]\,E_0 \qquad \text{Where } \gamma = \frac{1}{\sqrt{1-\frac{v^2}{c^2}}}$$

Hence, any one of the parameters can be found if rest of them are known.

When the beam passes through a thin solid foil then multiple ionization and capture processes produce the spectra to be analyzed. X-rays emitted from foil excited beam are allowed to pass through soller slits. An absorber is placed between Sollar slit assembly and the detector which has an absorption edge just below the energy of the emitted photon. The angle θ is varied through the region where the Doppler shifted energy matches and then surpasses the threshold necessary for absorption.

For proper choice of thickness i.e. for preventing X-ray to be absorbed, the absorber is essentially transparent (or nearly so) at angle below the critical angle (where the resonance takes place, i.e. E_{ab} = Doppler Tuned E_0). Thus the intensity of line of interest will be drastically curtailed when its energy matches or exceeds the absorption edge energy. The total yield in the detector, such as proportional counter will reflect that loss. The dispersion properties of this spectrometer are contained entirely in Doppler formula

$$E_{ab} = \gamma\,[1- (v/c)\cos\theta]\,E_0$$

The form of above equation is preferred since we wish to enter E_0 as a quantity dependent on E_{ab}, v/c and **θ.** Experimentally, we would usually hold two of these parameters constant, while varying the third, and waiting for a sudden change in counting rate when the above equation is satisfied. For instance, fixing E_{ab} at filter (K edge energy) and keeping v/c constant, would result in a fixed angle θ.

Resolution of DTS

This depends upon the knowledge of absorption edge and the angular collimation of X-ray. The efficiency is high compared to dispersive devices and is determined by attenuation of filter, detector efficiency and angular resolution (at soller slit). Expression for resolution can be obtained by differentiating above equation.

Thus resolution of DTS

$$\Delta E_{ab} = \gamma E_0 (v/c) \sin(\theta) \Delta\theta$$

Since absorption edges typically have widths (ΔE_{ab})? about a fraction of an electron volt so a resolution ~ 0.1% is possible. With present setup, we expect the resolution of 3eV at 6.8 keV which makes our experiment free from satellite blending.

DTS at NSC

At NSC, Doppler Tuned Spectrometer is planned to be setup at General Purpose Scattering Chamber (GPSC). The big size of chamber provides high resolution and two rotating arms provide a wide angular range required for DTS. Since GPSC is made for general purpose, therefore we have endeavored to make our system as two major units; one is spectrometer and other the target moving system. They may be dismantled and re-installed quickly so that any other work in GPSC won't be hampered at all.

In phase I, out of two one DTS assembly has been fabricated and is on the verge of test run. DTS assembly is itself a multi component setup, which consists of a proportional counter with both position and energy resolution; a unique component called soller slit plate and several other supporting components. The assembly is shown in fig.1.

The entire assembly is made up on a 200 x 200 x 6 mm SS plate called ground plate, which has a notch at the bottom side, which will be exactly fit in the central slot on the rotating arm of GPSC. Above it another plate is placed called bottom plate, on which proportional counter is kept. X-rays coming out of absorber foil is counted by a gas counter working in proportional region. Here we have kept both, constant gas flow and gas without flow options open. One gas inlet and one gas outlet is provided so that constant gas flow could be made possible. This detector is placed after absorber foil having detection area of 25x200 mm and ionization length 47 mm. X-ray enters in the proportional counter via a 6 micron mylar (polypropylene) foil. When it passes through isobutane gas it is ionized and a current is induced which will finally go through the electronic equipments. Triangular anode has been chosen for getting position vis a vis angular sensitivity.

In front of proportional counter, another important component called absorber plate is placed in the proper slot made in the bottom plate, which hold different foil of different x-ray absorption edge. Foils are made up of thin layer of some material for which the absorption edge is very sharp. This acts as a radiation filter. Its principle is very basic. Every material has the property to absorb a particular radiation. Other radiations will just passes through it. For better resolution, sharp absorption edge is required. When ever absorber will absorb a photon, the detector will not get any photon and hence a dip will be produced in DTS spectra.

After the absorber plate, again a 200 x 100 x 5 SS plate, called supporting plate, is placed which provides support to the glass slides. Just above it two soller slit plate of same size is kept, which consists of 41 radial slots of 80 X 1.5 mm with angular separation of 0.37^0. The centre of GPSC is considered to be its centre. These slots are made using CNC wire cutting machine for high precision. In between these two soller slit plates, glass slides of 80x20x1.5 have been placed. These provide different channels for x-ray photons. Above proportional counter another 200x200x6 mm SS plate called top plate is kept, which provides support to the upper soller slit plate. For preventing the background cosmic radiation from reaching the proportional counter, lead shielding with proper thickness has been provided to the counter.

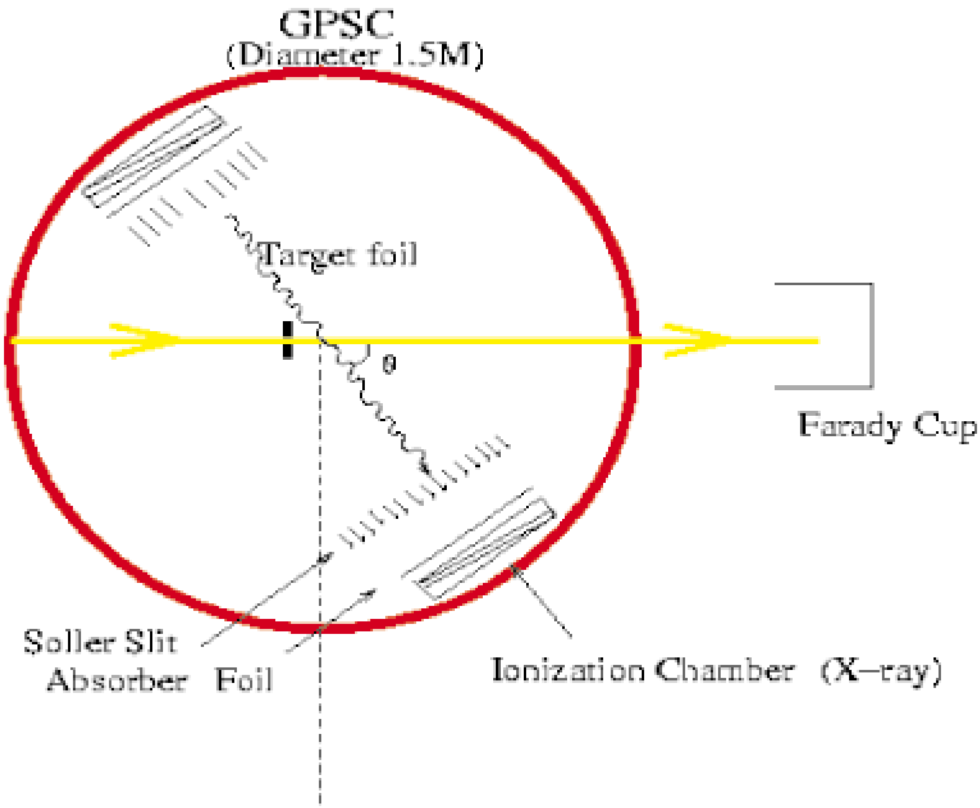

Fig. 1 : Geometrical Configuration of Doppler Tuned Spectroscopy

4.6 RADIATION BIOLOGY BEAM LINE

4.6.1 Status of the Radiation Biology Beam line

A. Sarma, A. Kothari, R. Joshi, M. Sota, Rakesh Kumar and P. Barua

The specially designed beam line can deliver beams of proton, ^7Li, ^{11}B, ^{12}C, ^{14}N and ^{16}O. The flux can be controlled from 10^2 particles/sec/cm^2 to 10^6 particles/sec/cm^2.

The radiation field is having 30 mm diameter with better than 97% uniformity. The flux control is done by adjusting a double slit through CAMAC from control room. A preset controller for faraday cup ensures the exposure repetition as per user requirement.

A major redesigning of the irradiation system is going to take place in near future, which would take care of the remote handling of petri dishes in an enclosed sanitised environment during irradiation, multiple irradiations of one sample after another without losing time and keeping the petri dishes in the medium when they are not being irradiated. The dosimetry system would also be improvised along with that. The renovation would facilitate better experimental condition from the biological point of view.

The Faraday cup FC L1-1 in the beam line had been malfunctioning and it was not reading beam current correctly. The cup assembly has been changed.

4.6.2 Status of the Molecular Radiation Biology Laboratory

A. Sarma

The laboratory is designed to extend user support to the best possible way during experiments. The experiments that are undertaken recently require suitable in-house facilities for relevant protocols. Apart from the normal equipment like microbalance, autoclave, bio-safety cabinet, oven, refrigerated centrifuge, PCR machine, Gel Doc, AFIGE system and Semi dry transblotter etc., we have installed a -80° C Ultra Freezer [Heto] and a -20° C Deep Freezer [Vest Frost]. Apart from these, a fluorescent microscope [Carl Zeiss] has been installed to facilitate the experiments based on FISH and immunofluorescent assays. A Coulter Cell counter is planed to be procured.